Ore Geology Reviews 95 (2018) 639–648

Contents lists available at ScienceDirect

Ore Geology Reviews

journal homepage: www.elsevier.com/locate/oregeorev

Variations in Zn and S isotope chemistry of sedimentary sphalerite, Wusihe Zn-Pb deposit, Sichuan Province, China

Chuanwei Zhu[a], Shili Liao[b], Wei Wang[c,d], Yuxu Zhang[a], Tao Yang[e], Haifeng Fan[a], Hanjie Wen[a,f,*]

[a] State Key Laboratory of Ore Deposit Geochemistry, Institute of Geochemistry, Chinese Academy of Sciences, Guiyang 550081, Guizhou, China
[b] Key Laboratory of Submarine Geosciences, Second Institute of Oceanography, SOA, Hangzhou 310012, Zhejiang, China
[c] The 117 Geological Brigade of Guizhou Bureau of Geology and Mineral Exploration and Development, Guiyang 550018, Guizhou, China
[d] China University of Geosciences, Wuhan 430074, Hubei, China
[e] State Key Laboratory for Mineral Deposits Research, Department of Earth Sciences, Nanjing University, Nanjing 210093, Jiangsu, China
[f] University of Chinese Academy of Sciences, Beijing 100049, China

ARTICLE INFO

Keywords:
Zn-S isotopes
Isotope fractionation
SEDEX hydrothermal system
Wusihe Zn-Pb deposit
Sichuan-Yunnan-Guizhou area

ABSTRACT

The Sichuan–Yunnan–Guizhou (SYG) metallogenic province, southwestern China, is one of the largest Zn-Pb producers in the world. The Zn-Pb deposits in this area have been studied over many years and are commonly classified as Mississippi Valley Type (MVT) deposits. We investigated geological and mineralogical features of the Wusihe deposit and found that ores formed at the sedimentary metallogenic stage exhibit banded and normal grading textures and have different mineral assemblages from other deposits in this area. These features have not been reported previously, suggesting special formation mechanisms for these sedimentary ores. In this study, we firstly investigate the isotope geochemistry of Zn and S in syngenetic sphalerite from the Wusihe deposit. We elucidate spatial and temporal variations of Zn and S isotopes to provide a better understanding for Zn and S isotope fractionation during the hydrothermal processes. The $\delta^{34}S_{CDT}$ values of microdrilled sphalerite range from 9.4‰ to 20.9‰ (mean = 14.3‰), which are ca.15‰ lower than that of sulfate from the Dengying Formation, suggesting that reduced sulfur in sphalerite formed through thermochemical sulfate reduction (TSR) but not microbial sulfate reduction (MSR). At the hand specimen scale, no significant Zn isotopic fractionation was observed from bottom to top of the banded sphalerite ore and we propose a model that Zn isotopes are homogeneous in Zn-bearing hydrothermal fluid, and Zn^{2+} was rapidly and completely precipitated to form sphalerite. This process results in minor Zn isotopic variations in sphalerite ($\Delta^{66}Zn$ = 0.08‰) and initial hydrothermal fluid composition was calculated to be $\delta^{66}Zn$ values = 0.37 ± 0.03‰. By contrast, positive linear relationships were observed in the sphalerite ore with normal grading between $\delta^{66}Zn$ and $\delta^{34}S_{CDT}$ values and between $\delta^{34}S_{CDT}$ values and Zn/Cd ratios, which are not reported previously. Combined with previous studies, it is proposed that the variations in fluid temperatures may be the key factor that results in such positive correlations.

In addition, this study gives some new insights into geochemical and isotopic behavior of Zn and S in hydrothermal systems, and provides an initial glimpse into the utilization of Zn isotopes as an environmental tracer for reconstruction of Zn isotope compositions in the Ediacaran Ocean.

1. Introduction

In natural, zinc (Zn) has five stable isotopes, including ^{64}Zn (48.63%), ^{66}Zn (27.90%), ^{67}Zn (4.10%), ^{68}Zn (18.75%), and ^{70}Zn (0.62%) (Rosman, 1972). With the development of multi collector-inductively coupled plasma-mass spectrometry (MC-ICP-MS), zinc isotope analytical precision has been significantly improved. This opened a new opportunity for cycling of Zn by detecting minor changes in its isotopic composition in nature, which then allowed the geological processes responsible for these variations to be elucidated (e.g., Mason et al., 2005; Toutain et al., 2008; Cloquet et al., 2008; Zhou et al., 2014a,b; Liu et al., 2016, 2017; Duan et al., 2016; Wang et al., 2017). Due to high Zn abundance and well-constrained formation conditions, ore deposits, especially for Zn-Pb deposits, are considered particularly suitable for studies of Zn isotope fractionation. Consequently, much of the research over the last fifteen years conducted preliminary investigations of Zn

* Corresponding author at: State Key Lab of Ore Deposit Geochemistry, Institute of Geochemistry, Chinese Academy of Sciences, 99 Linchengxilu Road, Guiyang, 550081, Guizhou Province, China.
E-mail address: wenhanjie@vip.gyig.ac.cn (H. Wen).

https://doi.org/10.1016/j.oregeorev.2018.03.018
Received 25 August 2017; Received in revised form 14 March 2018; Accepted 19 March 2018
Available online 20 March 2018
0169-1368/

isotope fractionations and possible controlling mechanisms in different types of Zn-Pb deposits, which include (1) sedimentary exhalative (SEDEX), (2) Mississippi Valley Type (MVT), (3) volcanic-hosted massive sulfide (VHMS), and (4) magmatic-hydrothermal related ore deposits. These studies predominantly focused on sulfides and demonstrated that variations in Zn isotopes appear to be triggered by (1) changess in geochemical conditions (Fujii et al., 2011; Pašava et al., 2014), (2) mixing of multiple Zn sources (Wilkinson et al., 2005), and (3) kinetic fractionation during sphalerite precipitation (Kelley et al., 2009; Gagnevin et al., 2012; Zhou et al., 2014a,b). It is thus that Zn isotopes were used to better understand the geochemical processes of metal sources, transportation and deposition in such hydrothermal systems.

As one of the largest base metal sources in China, the Sichuan–Yunnan–Guizhou (SYG) metallogenic area contains over four hundred of Zn-Pb deposits with total Zn and Pb ore reserves of more than 150 million tons (Mt) (Zhou et al., 2014a,b; Wang et al., 2014; Huang et al., 2004; Han et al., 2007; Zhang et al., 2015). Geological investigations demonstrated that Zn-Pb deposits in this area are carbonate-hosted deposits and were thought to be MVT deposits (Zaw et al., 2007; Han et al., 2007; Ye et al., 2011; Zhang et al., 2015), of which the formation conditions are already well established, providing essential subjects for the application of Zn isotope (Wu, 2013; Zhou et al., 2014a,b; He et al., 2016). However, many deposits, such as the Wusihe deposit, display quite different geological and geochemical characteristics from those of typical MVT deposits in this area (Zheng, 2012; Zhu et al., 2013, 2016; Wang et al., 2014; Wang, 2015), suggesting that the ore genesis of some Zn-Pb deposits in the SYG area could not be classified as MVT type deposits alone.

In our study, we evaluate the Wusihe deposit to elucidate spatial and temporal variations of Zn, Pb and S isotopes in ores, which are formed at sedimentary metallogenic stage. By taking samples of stratiform and grain sphalerite, we are able to examine processes of Zn, Pb and S isotopic fractionation within small scales and give assessments on metal sources and ore genesis of the Wusihe deposit. Meanwhile, utilizing Zn and S stable isotopes allows us to better understand sources, ore genesis and processing pathways that offer insights in the geochemical behavior of Zn and S in the Zn-Pb deposits from the SYG area.

2. Geological setting and sampling

The Wusihe deposit is located in the northwestern part of the SYG metallogenic province at the northwestern margin of the Yangtze Craton, where the strata consist of crystalline basements and sedimentary rocks (Fig. 1). Previous studies described the strata in the SYG area in detail (Zhou et al., 2001; Huang et al., 2004; Zhou et al., 2014a,b; Zhang et al., 2015; Zhu et al., 2017). Generally, the crystalline basements are comprised of (from lower to upper) the Lower Proterozoic Kangding Group (Pt_1^1k, migmatite and gneiss) and the Dahongshan Group (Pt_1^2d, meta-clastic rock and spilite-keratophyre sequence), and the Middle-Upper Proterozioc Kunyang Group ($Pt_{2\text{-}3}k$, clastic rock with minor carbonate). The sedimentary rocks include (from lower to upper) Sinian to Quaternary strata that mainly consist of limestone and dolomite. In addition, the largest igneous event in the SYG area is the Emeishan flood basalts (Late Permian), which cover an area of over 250,000 km^2 with a total thickness up to several hundred meters to 5 km (Zhou et al., 2001).

The strata exposed in the Wusihe ore field are mainly composed of (from lower to upper) Mesoproterozoic granitoids (γ), Mesoproterozoic Ebian Group (Pt_2eb; clastic rocks and carbonate rocks; coeval with the Kunyang Group; Xiong et al., 2013), Lower Sinian (Ediacaran) Suxiong Formation (Z_1s; volcanic rocks), Upper Sinian (Ediacaran) Dengying Formation (Z_2d; carbonates), Cambrian clastic and carbonate, Ordovician sandstone, Silurian shale, and Permian limestone (Fig. 1) (Zheng, 2012; Wang, 2015; Xiong et al., 2016). The deposit is hosted in the Upper Sinian (Ediacaran) Dengying Formation, which mainly consists of silica dolomite. The main fold axial, namely the Wanlicun syncline, trace strikes 5-16°east and 4-22° north with an angular cross fold aligned ~ 180° (north to south); the main faults are the NW-trending Matuo fault (F1) and the NE-trending Wangmaoshan fault (F2) (Fig. 1).

The demonstrated reserves in the Wusihe deposit are more than 10 Mt (Zn + Pb) ore at grades of ~10.58% (Zn + Pb) (Zheng, 2012), associated with other accompanying elements such as Ag, Ge, and Cd. The geological features of the Wusihe deposit were summarized by Zheng (2012) and Wang (2015). Geological investigations demonstrated that the Wusihe deposit is mainly present in the Wanlicun syncline within an area about 3.7 km long and 2.5 km wide (Fig. 1). Orebodies predominantly exhibit stratabound and lenticular in shape and parallel to the bedding of the host rocks (Fig. 2). The ores are dominantly sulfides with relatively simple mineral association, in which sphalerite is the most abundant economic mineral; in contrast, galena and pyrite are minor. Gangue minerals are primarily quartz and dolomite with minor organic matter (bitumen), apatite, rutile and calcite (Fig. 3). To our knowledge, apatite and rutile have not been previously reported in ores from these Zn-Pb deposits in the SYG area. Broadly, the mineralization has been divided into two stages, which are (I) sedimentary metallogenic stage, sphalerite exhibiting banded and normal grading; and (II) hydrothermal ore-forming stage, breccia and veined sphalerite, commonly accompanied by galena, pyrite and quartz. It is thus that the ores are divided into two major types on the basis of their origins, including sedimentary ores (stage I) and replaced ores (stage II), which predominantly exhibit laminated, banded, spotted, breccia, veined, and disseminated structure. In this study, we only investigate ores from sedimentary metallogenic stage (stage I), in which geochemical signatures are well preserved and are not affected by hydrothermal fluid from stage II (Xiong et al., 2016). This conclusion can be proved by detailed electron microscope analysis (Wang, 2015).

3. Samples and methods

3.1. Microsampling

In this study, we investigate spatial and temporal variations of Zn, Pb and S isotopes in syngenetic sphalerite. Two representative hand specimens, namely WSH-65 and WSH-95 (Figs. 2 and 3), were collected from lower and upper sedimentary orebody, respectively. The economic minerals of these two samples only comprise sphalerite; gangue minerals include quartz and organic matter (bitumen). Sphalerite in sample WSH-65 shows colloform and banded texture with grain size of ~0.1 mm; in contrast, sphalerite in sample WSH-95 shows well-defined and various grain sizes, which systematically decrease (lower to upper) from ca. 1 cm to ca. 0.1 cm, indicating the deposition rate increased upwards. The two hand specimens display different textures of paragenesis minerals and grain size of sphalerite. Quartz in WSH-65 is a dominant mineral, while quartz in WSH-95 is present in the space between sphalerite grains (Figs. 2 and 3).

Sampling of syngenetic sphalerite for Zn, Pb and S isotope analysis has been carried out using a Microdrill sampling system (Relion MSS IV; USA) with the drill diameter of 1 mm (tungsten carbide-tipped drill steel). Samples for microdrilling were randomly targeted at sphalerite concentrated area from the bottom to the top of the studied hand specimens. Care was taken to sample sphalerite that was visually free of other minerals. Minute crystals of quartz could not be avoided during microsampling; however, gangue minerals would have negligible effect on Zn, Pb and S isotope ratios in comparison with that of sphalerite.

3.2. Zn and Pb separation

Prior to Zn isotopic analysis, sphalerite micro-samples were chemically purified on columns containing 3 mL of pre-cleaned 100–200 mesh AG MP-1M anion-exchange resin, using a protocol adapted from Pallavicini et al. (2014). Samples were individually transferred into a

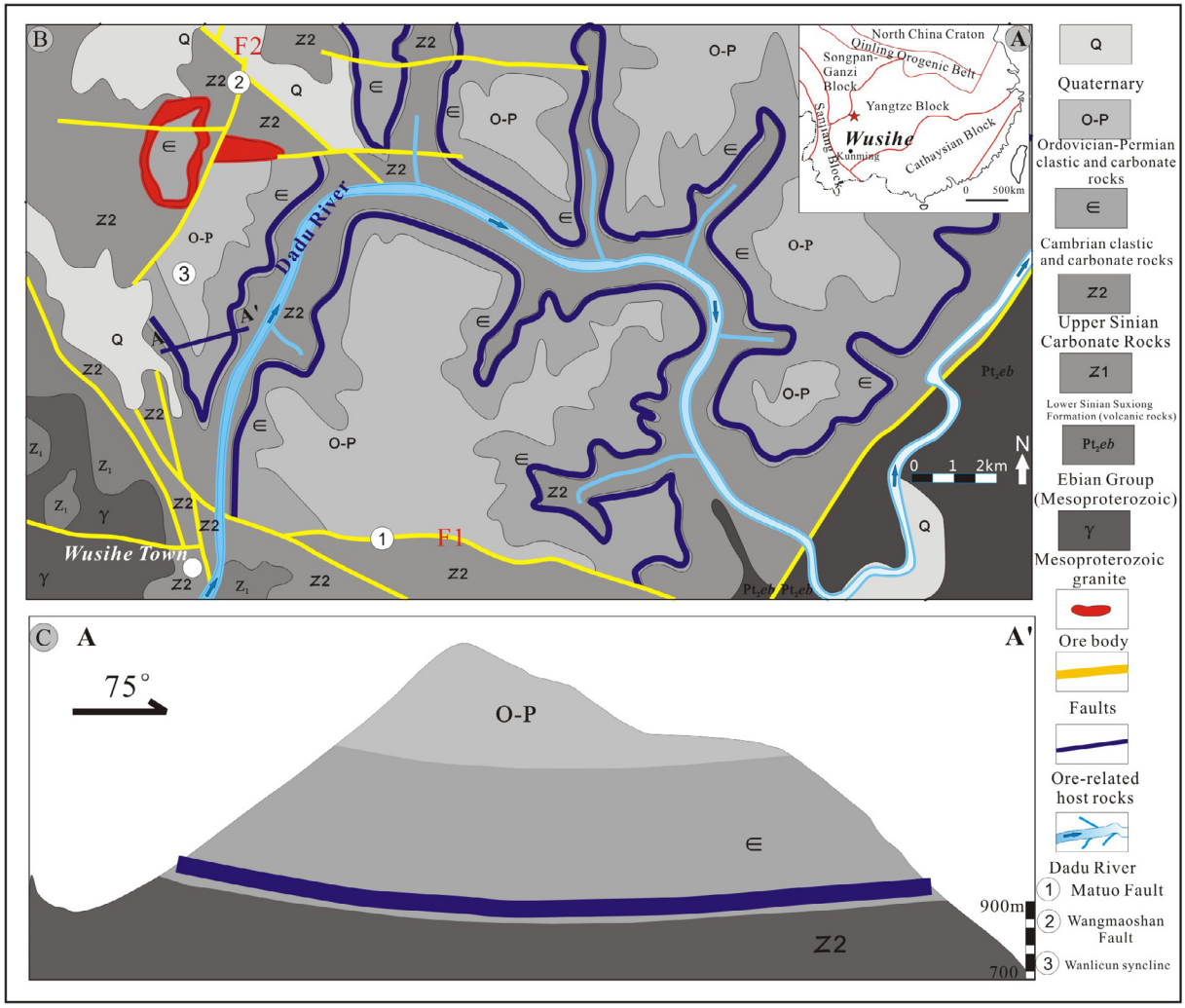

Fig. 1. (A) Sketch of tectonic framework of the South China; (B) Regional geological map of the Wusihe district; (C) Cross-section through the Wusihe deposit (Modified from Wang, 2015).

7 mL Teflon digestion vial (Savilex; USA), and then reacted with 1 mL of concentrated HNO_3 at 110 °C for about 24 h. After dryness, each sample was digested using 0.1 mL of concentrated HF, and then heated at 110 °C until dryness. Finally, 5 mL of 1% HNO_3 (v/v) were added and the solution was transferred into a 15 mL polypropylene centrifuge tube. After centrifugation, 2 mL supernatant were transferred for major and trace element measurements to monitor recoveries of both Zn and Pb, while another 2 mL supernatant were transferred for chemical purification. Before chemical purification, the 2 mL supernatant were evaporated to dryness at 110 °C followed by adding 2 mL of 2 N HCl. After the adsorption of metals onto the column,10 mL of 2 N HCl were passed through the columns. The Pb, Zn and Cd were then eluted by using 12 mL of 0.3 N HCl, 12 mL of 0.012 N HCl, and 24 mL 0.0012 N HCl, respectively. The solution was evaporated to dryness at 110 °C and then dissolved in 2 mL of 1% HNO_3. Additionally, 0.5 mL of the final solution was used for Pb, Zn and Cd measurements to monitor their recoveries, while the residue was then used for Pb and Zn isotope analysis. Full recoveries of Pb and Zn were monitored by comparing between unprocessed and processed of each samples, and found to be complete ~100% and > 98%, respectively.

3.3. Mass spectrometric measurements

An inductively coupled plasma optical emission spectrometer (ICP-OES; Varian Vista MPX) was employed to measure the concentrations of major and trace elements.

Isotopic Zn ratios were analyzed using a Thermo Scientific Neptune Plus MC-ICP-MS instrument at the State Key Laboratory of Crust–Mantle Evolution and Mineralization at Nanjing University. Instrumental mass bias correction of Zn isotopes was achieved through a coupled method of sample-standard bracketing (SSB) and Cu-doping, and the Faraday cups were aligned to measure ^{63}Cu (L3), ^{64}Zn (L2), ^{65}Cu (L1), ^{66}Zn (centre cup), ^{67}Zn (H1), ^{68}Zn (H2), and ^{70}Zn (H4) isotopes. The concentrations of Zn and Cu in samples and standards were diluted to 1.0 μg/g and 0.5 μg/g using 1% HNO_3 (v/v), and they were prepared to the same concentration to within a 10% difference. Both samples and standards were analyzed at an uptake rate of ~100 μL/min, and generally yielded a total Zn voltage of ~28.8 V. All samples and standard solutions were run in three blocks with 15 cycles per block. The nebulizer and spray chamber were washed after each run using 5% HNO_3(v/v) until the voltage reached the original background level (~3 min). In this study, Zn isotopic ratios are expressed in standard delta notation in per mil units relative to the IRMM 3702 Zn solution during measurements, as defined by the following relationship:

$$\delta^{x/64}Zn(‰) = [(^{x}Zn/^{64}Zn)_{sample}/(^{x}Zn/^{64}Zn)_{IRMM3702} - 1] \times 1000$$

where ^{x}Zn represents the ^{66}Zn, ^{67}Zn, ^{68}Zn and ^{70}Zn isotopes.

The CAGS-1 Zn standard solution was suggested to use as a secondary reference material, of which the analysis yields an average $\delta^{66}Zn_{\ IRMM\ \ 3702} = -0.84 \pm 0.03‰$ (n = 6) that consistent with

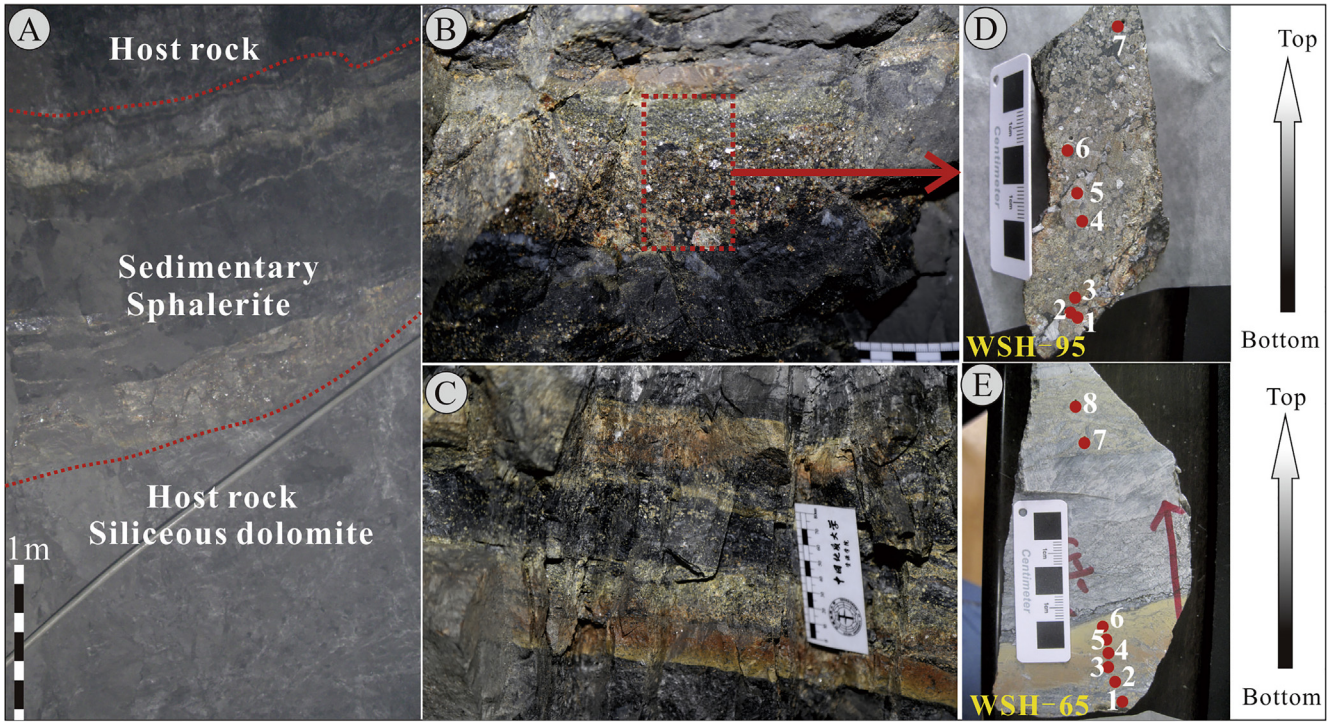

Fig. 2. (A) Field photograph of ore-body (sedimentary sphalerite); (B) Specimen photograph showing normal grading; (C) Specimen photograph showing banded sphalerite; (D) Specimen photograph of WSH-95 with sampling sites, grain size of sphalerite increases from the bottom to the top; (E) Specimen photograph of sample WSH-65 with sampling sites, banded sphalerite.

previous reported values ($\delta^{66}Zn_{\ IRMM\ 3702} = -0.77 \pm 0.10‰$; Tang et al., 2016). At present, the Johnson Matthey (JMC) Zn "Lyon solution" is an accepted international Zn isotope standard. Thus, Zn isotopic data in this study are also reported relative to the JMC Zn isotope standard using the equation expressed as $\delta^{66}Zn_{JMC} = \delta^{66}Zn_{IRMM\ 3702} + 0.27$ (Wang et al., 2017), and Zn isotopic data in this study are discussed relative to the JMC.

Sulfur isotope ratio measurements were determined using a Thermo Finnigan MAT 253 isotope ratio mass spectrometer (Thermo Scientific, Bremen, Germany) at the State Key Laboratory of Ore Deposit Geochemistry, Institute of Geochemistry, Chinese Academy of Sciences. The standard reference materials (Ag_2S) for sulfur isotope measurement were IAEA-S-1 (reference material 8554; $\delta^{34}S_{CDT} = 0.3‰$), IAEA-S-2 (reference material 8555; $\delta^{34}S_{CDT} = 22.62 \pm 0.17‰$), and IAEA-S-3 (reference material 8529; $\delta^{34}S_{CDT} = -32.49 \pm 0.17‰$), which yielded a relative error of < 0.2‰ (all errors are 2 sigma of the standard error). All of the S isotopic data are reported relative to the Canyon Diablo Troilite (CDT).

Isotopic ratios of $^{206}Pb/^{204}Pb$, $^{207}Pb/^{204}Pb$ and $^{208}Pb/^{204}Pb$ were measured on a Thermo Scientific Neptune Plus MC-ICP-MS instrument at the State Key Laboratory of Crust–Mantle Evolution and Mineralization at Nanjing University. A method of standard bracketing coupled with Tl (NIST-997)-doping on standard NIST-981 was adopted for Pb isotopic analyses. Repeated analyses of Pb standard (NIST NBS-981) yielded a $^{206}Pb/^{204}Pb$ ratio of 16.9333 ± 0.0006 (1SD), a $^{207}Pb/^{204}Pb$ ratio of 15.4871 ± 0.0005 (1SD) and a $^{208}Pb/^{204}Pb$ ratio of 36.6840 ± 0.0013 (1SD), which are consistent with the reference values reported by Yuan et al. (2016) for NIST NBS-981 ($^{206}Pb/^{204}Pb = 16.9405$, $^{207}Pb/^{204}Pb = 15.4963$ and $^{208}Pb/^{204}Pb = 36.7219$).

4. Results

Due to limited amount of available weights of microdrilled samples (~15 mg), it is difficult to obtain the weights of each sample with high precision. We measured Zn, Pb and Cd concentrations in both the digested solution and purified solution to monitor the recoveries of target elements during chemical separation. It is thus that we only report the Zn/Cd ratios of the studied samples as listed in Table 1.

Zn isotope compositions of the studied sphalerite are reported in Table 1, together with their S and Pb isotopic ratios. Microdrilled sphalerite from sample WSH-65 has minor Zn isotopic fractionation with $\delta^{66}Zn$ values ranging from +0.32‰ to 0.40‰ (Fig. 4), while microdrilled sphalerite from sample WSH-95 has relatively larger Zn isotope fractionation than that of sample WSH-65 with $\delta^{66}Zn$ values ranging from +0.05‰ to +0.34‰ (Fig. 5). Similarly, the variations in Pb isotopic composition in sample WSH-65 are small, with $^{206/204}Pb$, $^{207/204}Pb$, and $^{208/204}Pb$ ranging from 18.2008 to 18.2783, 15.6551 to 15.6762, and 38.3100 to 38.4583, respectively (Table 1). Pb isotopic compositions of sample WSH-95 have relatively large variations in comparison with that of sample WSH-65, with $^{206/204}Pb$, $^{207/204}Pb$, and $^{208/204}Pb$ ranging from 17.9821 to 18.3329, 15.6335 to 15.6837, and 38.0458 to 38.4441, respectively (Table 1). The $\delta^{34}S_{CDT}$ values of sample WSH-95 occupy a narrow range between +9.4‰ and +12.9‰ with an average value of +10.9‰ (Fig. 5). By contrast, the variations of sulfur isotope compositions of sphalerite from sample WSH-65 are much larger than those from sample WSH-95 with $\delta^{34}S_{CDT}$ values ranging from +13.2 to +20.9‰ (mean = +17.2‰) (Fig. 4). Sample WSH-95 displays Zn/Cd ratios ranging from 118 to 377 (mean = 224). By contrast, samples WSH-65 shows higher Zn/Cd ratios than that of WSH-95 ranging from 280 to 476 (mean = 364) (Figs. 4 and 5).

5. Discussion

5.1. Possible formation mechanisms for samples WSH-65 and WSH-95

At present, Zn isotopic signatures in different types of Zn-Pb deposits have been well-defined, including MVT, VHMS, SEDEX, magma-related and Irish-type Zn-Pb deposits (Duan et al., 2016, and references therein). However, the $\delta^{66}Zn$ values of sphalerite from those deposits overlap significantly, indicating that the use of Zn isotopes as potential

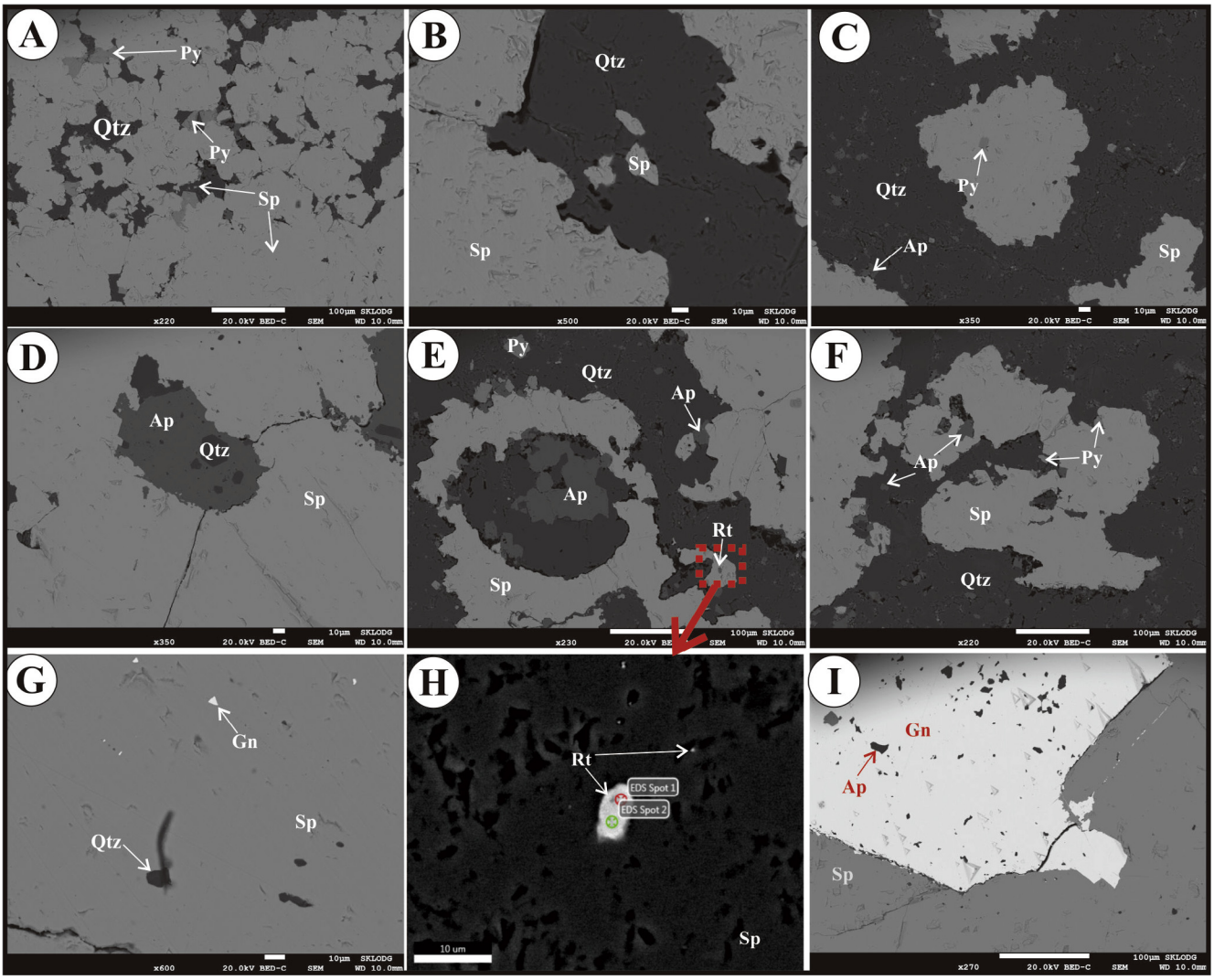

Fig. 3. Back-scatter electron (BSE) images showing aspects of sample WSH-65 (A-C) and sample WSH-95 (D-I). (A) Micro-inclusions of pyrite (Py) and quartz (Qtz) in sphalerite (Sp); (B) Sphalerite intergrowths with quartz associated with micro-inclusions of sphalerite in quartz; (C) Quartz-sphalerite assemblage with small micro-inclusions of pyrite and apatite (Ap); (D) euhedral crystalline quartz in sub-euhedral apatite; (E) Quartz-sphalerite assemblage with micro-inclusions of euhedral pyrite and xenomorphic rutile (Rt); (F) Small disseminated pyrite and apatite occur in quartz and sphalerite; (G) Triangular galena (Gn) exsolutions in sphalerite; (H) Erratic rutile occurs in sphalerite; (I) later sub-euhedral galena intergrowths with sphalerite and contains small micro-inclusions of apatite.

Table 1
Zinc, sulfur and lead isotopic compositions coupled with Zn/Cd ratio in the samples from the Wusihe deposit.

Sample No.	$^{206/204}$Pb	$^{207/204}$Pb	$^{208/204}$Pb	$\delta^{66}Zn_{IRMM\ 3702}$	2SD	$\delta^{66/64}Zn_{JMC}$	2SD	$\delta^{34}S_{CDT}$	Zn/Cd
WSH-95-1	18.3329	15.6837	38.4441	−0.09	0.01	0.18	0.01	10.8	202
WSH-95-2	17.9935	15.6350	38.0921	−0.03	0.01	0.24	0.01	11.7	252
WSH-95-3	17.9821	15.6335	38.0615	−0.04	0.01	0.23	0.01	9.8	171
WSH-95-4	17.9896	15.6388	38.0458	−0.22	0.03	0.05	0.03	9.4	118
WSH-95-5	18.0155	15.6396	38.0855	−0.04	0.09	0.23	0.09	11.8	296
WSH-95-6	17.9965	15.6394	38.0637	−0.07	0.03	0.20	0.03	10.0	150
WSH-95-7	18.1302	15.6664	38.2268	0.07	0.01	0.34	0.01	12.9	377
WSH-65-1	18.3503	15.6728	38.4206	0.05	0.02	0.32	0.02	13.2	280
WSH-65-2	18.2008	15.6606	38.3136	0.13	0.03	0.40	0.03	14.5	415
WSH-65-3	18.2783	15.6762	38.4583	0.09	0.06	0.36	0.06	20.6	353
WSH-65-4	18.2067	15.6551	38.3100	0.11	0.01	0.38	0.01	20.9	319
WSH-65-5	18.2476	15.6606	38.3358	0.10	0.03	0.37	0.03	20.7	318
WSH-65-6	18.2636	15.6628	38.3409	0.10	0.03	0.37	0.03	17.4	322
WSH-65-7	18.2458	15.6663	38.3146	0.10	0.02	0.37	0.02	16.7	476
WSH-65-8	18.2466	15.6675	38.3174	0.13	0.01	0.40	0.01	13.5	427

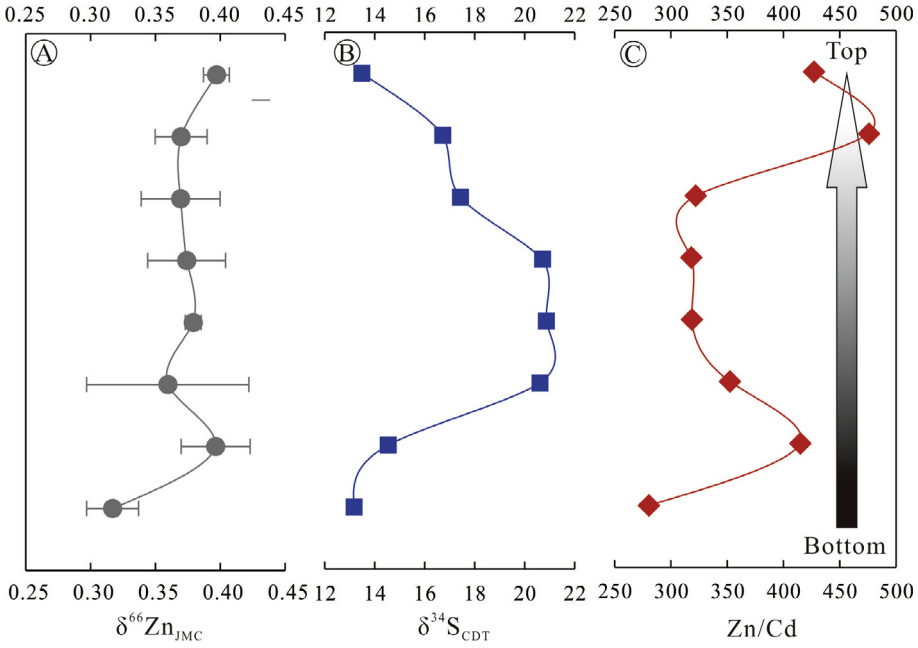

Fig. 4. $\delta^{66}Zn$, $\delta^{34}S$ and Zn/Cd ratios in sphalerite from the bottom to the top of sample WSH-65.

geochemical proxies to classify the corresponding Zn-Pb deposits represents a major challenge. Geological investigations demonstrate that sphalerite from the sedimentary stage is coeval with the host rocks, suggesting the origins of the sphalerite may be similar to that of seafloor sulfide and/or SEDEX type sphalerite. In Wusihe, the Zn isotope compositions of the original hydrothermal fluid are calculated to be 0.37 ± 0.03‰ (see below), which is quite different from the reported high-T and low-T seafloor hydrothermal fluids from mid-ocean ridge systems (0.21 ± 0.04‰ and 1.01 ± 0.04‰; John et al., 2008). Due to small isotope fractionation during sulfide precipitation, we propose that the origin of syngenetic sphalerite from Wusihe are different from that of seafloor sulfide. This conclusion is consistent with geological mapping indicating that no related igneous rocks occur in the Wusihe district (Zheng, 2012; Wang, 2015; Xiong et al., 2016). Kelley et al. (2009) and Gao et al. (2017) reported Zn isotope compositions of sphalerite from the Red Dog deposit and the Dongshengmiao deposit, respectively, which are typical SEDEX type deposits. The $\delta^{66}Zn$ values of the Wusihe sphalerite range from 0.05 to 0.40‰, which are consistent with the results of sphalerite from the Red Dog deposit (0.00‰ to 0.60‰) and the Dongshengmiao deposit (0.17‰ to 0.40‰). Based upon geological settings and Zn isotopic signatures of sphalerite, we propose that the origin of syngenetic sphalerite in the Wusihe deposit is similar to that of SEDEX type sphalerite.

5.1.1. Zn and sulfur isotope variations in sample WSH-65

Two processes are considered to account for the reduced sulfur in sulfides from hydrothermal systems: (1) microbial sulfate reduction (MSR); and (2) thermochemical sulfate reduction (TSR). These two processes could result in large sulfur isotopic fractionations, which have been well-defined in previous studies (Rollinson, 1993; Strauss, 1997;

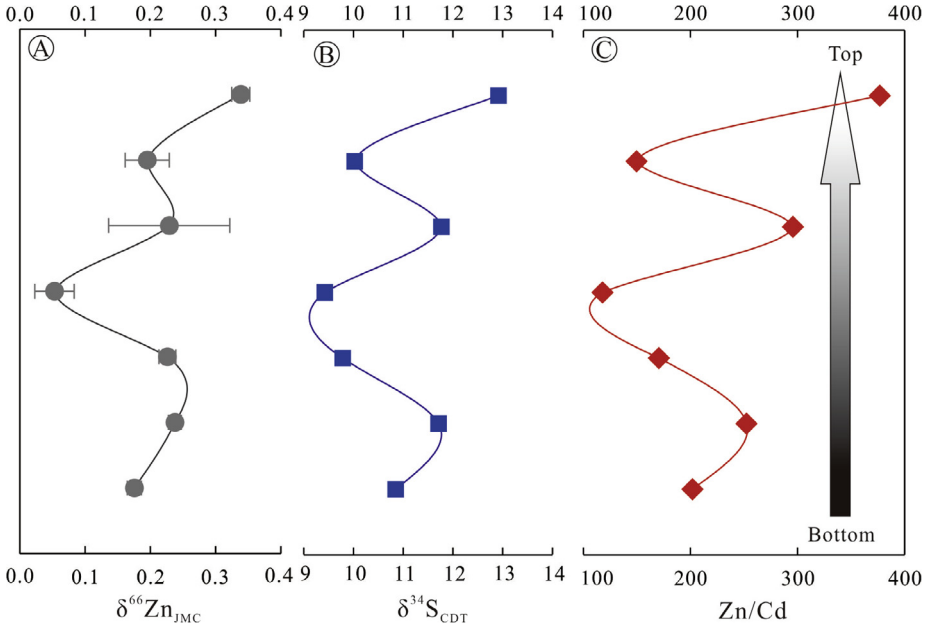

Fig. 5. Variations in $\delta^{66}Zn$ (A), $\delta^{34}S$ (B) and Zn/Cd ratios (C) in sphalerite from the bottom to the top of hand specimen WSH-95.

Lefticariu et al., 2017; Meshoulam and Amrani, 2017). Generally, experimentally determined $\Delta^{34}S_{SO4\text{-}H2S}$ values for TSR suggest kinetic fractionations of 20, 15, and 10‰ at 100 °C, 150 °C, and 200 °C, respectively (Machel et al. 1995). By contrast, a reaction of the MSR will produce sulfides depleted in $\delta^{34}S_{CDT}$ by ~72‰ relative to the parent sulfate (e.g., Lefticariu et al., 2017, and references therein). Previous studies have shown that the $\delta^{34}S_{CDT}$ values of sulfate from the Dengying Formation vary from 24.0‰ to 36.7‰, with an average value of 29.6‰ (Zhang et al., 2004; Goldberg et al., 2005). In the Wusihe deposit, the $\delta^{34}S_{CDT}$ values of microdrilled sphalerite range from 9.4‰ to 20.9‰ (mean = 14.3‰), which are ca.15‰ lower than those of sulfate from the Dengying Formation, suggesting that reduced sulfur in sulfides formed via TSR, instead of MSR. This conclusion is consistent with previous studies in the Wusihe deposit (Zheng, 2012; Wang, 2015; Xiong et al., 2016).

At present, two processes may be considered to account for the variations of $\delta^{34}S_{CDT}$ values in SEDEX deposits, including: (1) mixing between fluids (Gadd et al., 2017) and (2) kinetic fractionation during sulfide precipitation (Machel et al., 1995; Strauss, 1997; Böttcher et al., 1998). From the stratigraphic base to the top of sample WSH-65, the $\delta^{34}S_{CDT}$ values of microdrilled sphalerite increase systematically from 13.2‰ to 20.9‰, and then decrease from 20.9‰ to 13.5‰. This trend is extremely similar to that of layered sphalerite (3.9‰ to 14.6‰; D4, 21644A) from the Navan Zn-Pb deposit (Ireland) (Gagnevin et al., 2012). The latter authors proposed that the sulfur isotopic signatures of D4 represent sphalerites precipitated from mixing between hydrothermal (enriched in heavy sulfur isotopes) and bacteriogenic sulfur (enriched in light sulfur isotopes). Gadd et al. (2017) investigated the sulfur isotopic compositions in sulfide from a typical SEDEX deposit, showing that the sulfur isotope compositions of both sphalerite and galena progressively decreases from the stratigraphic base to the top, and the distinct sulfur isotopic signatures are interpreted to represent varying contributions of bacterially reduced seawater sulfate and thermochemically reduced seawater sulfate. In the Wusihe deposit, no bacteriogenic sulfide has been observed (e.g., framboidal pyrite) at present and reduced sulfur in the Wusihe is unlikely supplied through MSR as discussed above (Zheng, 2012; Wang et al., 2014; Wang, 2015). Furthermore, no significant Zn isotope fractionation was observed in microdrilled sphalerite and there is no obvious correlation between Zn and S isotope compositions in those samples (Fig. 6). If there were multiple Zn-bearing fluids, it is highly unlikely that we would only observe such an extremely narrow range of $\delta^{66}Zn$ variability (Wilkinson et al., 2005). It is thus clear that fluid mixing is not the key factor controlling observed variations in the Zn isotope composition, which reflects a homogenous source. Thus, a different mechanism must be responsible.

It is proposed that the ranges of sulfur isotope signatures result primarily from kinetic isotopic fractionation. In a closed (or partly closed) system, the concentration of the reactant sulfate in seawater decreases progressively and, due to the kinetic isotope effect involved, the $\delta^{34}S_{CDT}$ values of both reactant and product change with time (Rayleigh fractionation process) towards heavier $\delta^{34}S_{CDT}$ values (Strauss, 1997). In addition, the kinetic fractionation of sulfur isotopes during TSR is temperature dependent, and that lower temperatures result in larger fractionations between the parent sulfate and daughter sulfide, while higher temperatures result in smaller fractionations (Machel et al. 1995; Gadd et al., 2017). It is thus, the variations in $\delta^{34}S_{CDT}$ values in WSH-65 were induced by different precipitation temperatures.

We propose a model in which Zn isotopes are homogeneous in Zn-bearing hydrothermal fluid, and sphalerite precipitation took place in a system with $mH_2S > mZn^{2+}$, and then Zn^{2+} was rapidly and completely precipitated to form sphalerite. This process results in minor or no significant Zn isotopic fractionation in sphalerite. In addition, Pb isotopic data in WSH-65 also show a homogenous $^{206}Pb/^{204}Pb$ signature (mean = 18.255 ± 0.047), which suggests that the hydrothermal fluid is isotopically homogeneous and supports the precipitation model as proposed above. For these reasons it is highly likely that initial hydrothermal fluid composition has $\delta^{66}Zn$ values of 0.37 ± 0.03‰.

5.1.2. Zn and sulfur isotope variations in sample WSH-95

Zinc isotope fractionations are relatively large in WSH-95 ($\Delta^{66}Zn$ = 0.29‰) in comparison with those of WSH-65 ($\Delta^{66}Zn$ = 0.08‰). Interestingly, $\delta^{66}Zn$ values show a positive correlation with $\delta^{34}S_{CDT}$ values in WSH-95, while such relationship was not observed in WSH-65 (Figs. 6 and 7). These results suggest different formation origins between WSH-65 and WSH-95. Up to date, several processes have been well defined that result in Zn isotope fractionations in hydrothermal fluids, including: (1) changes in geochemical conditions (Fujii et al., 2011; Pašava et al., 2014); (2) mixing between fluids (Wilkinson et al., 2005); and (3) kinetic fractionation (Wilkinson et al., 2005; Gagnevin et al., 2012; Zhou et al., 2014a,b; Deng et al., 2016). Due to large amount of organic matters in the studied ores (Fig. 2), oxidized environments are a unlikely significant factor for the composition of Zn isotope in sphalerite, and it is more likely controlled by a reducing environment, thus ruling out hypothesis 1. Fluid mixing (hypothesis 2) is highly unlikely to account for such small variations in $\delta^{66}Zn$ values. Meanwhile, a homogeneous source of metal is supported by the relatively uniform Pb isotope composition of sphalerite from the Wusihe deposit with Pb isotope signatures being indistinguishable (average $^{206}Pb/^{204}Pb$ = 18.06 ± 0.13; Table 1). If there were multiple sources of Zn-mixing in the genesis of the Wusihe deposit, it is highly unlikely that we could only observe such a narrow range of $\delta^{66}Zn$, $^{206}Pb/^{204}Pb$ and $\delta^{34}S_{CDT}$ variability (Wilkinson et al., 2005; Gagnevin et al., 2012; Deng et al., 2016). It is thus that mixing of two or more metal sources is unlikely to be the key factor controlling spatial variations of Zn and S isotope composition, which largely reflects a

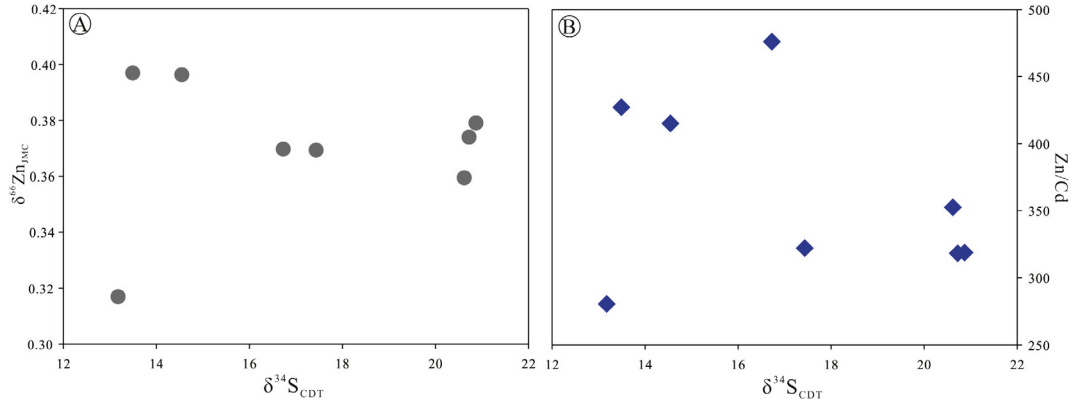

Fig. 6. Plots of $\delta^{66}Zn$ vs $\delta^{34}S$ (A) and Zn/Cd ratios vs $\delta^{34}S$ (B) in sphalerite from sample WSH-65.

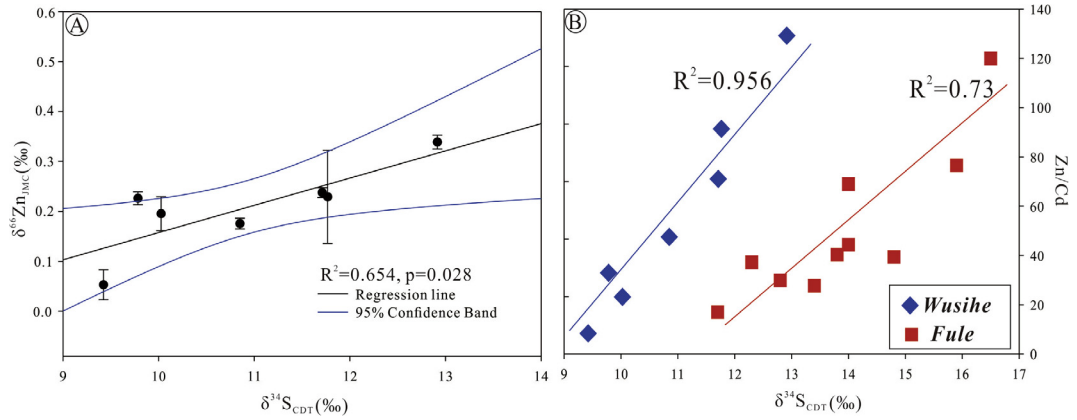

Fig. 7. Plots of $\delta^{66}Zn$ vs $\delta^{34}S$ (A) and Zn/Cd ratios vs $\delta^{34}S$ (B) in sphalerite from sample WSH-95. Data for the Fule deposit are from Zhu et al. (2017).

homogenous source. We propose that the ranges of Zn isotope signatures result primarily from kinetic isotopic fractionation. Previous studies have shown that light Zn preferentially partitions into the solid phase rather than the hydrothermal fluid, suggesting earlier precipitated sphalerite has lower $\delta^{66}Zn$ values (Wilkinson et al., 2005; Mason et al., 2005; Kelley et al., 2009; Gagnevin et al., 2012; Zhou et al., 2014a,b). Recent studies suggested that high $\delta^{66}Zn$ values are consistent with rapid precipitation of sphalerite at higher temperature (Pašava et al., 2014). Based upon S isotopic data and geological texture, we conclude that WSH-65 was precipitated rapidly at high temperatures while WSH-95 was precipitated slowly at low temperatures. Thus, the kinetic fractionation both of Zn and S isotopes during precipitation is temperature dependent kinetic isotope effect, which results in such a positive correlation between $\delta^{66}Zn$ and $\delta^{34}S_{CDT}$ values.

5.2. Zn/Cd ratios in microdrilled sphalerite

Schwartz (2000) and Wen et al. (2016) calculated Zn-Cd partitioning between liquid and coexisting sphalerite and suggested that the physico-chemical conditions of ore-forming fluids highly affected the Cd distribution in sphalerite such as reduced sulfur concentrations and fluid temperatures. However, according to the thermodynamic theory on the liquid-solid partitioning of Zn and Cd, the Zn/Cd ratios in sphalerite are the result of the competing influences of multiple parameters of the parent hydrothermal fluids (Schwartz, 2000; Wen et al., 2016). In this study, Zn/Cd ratios in sphalerite from sample WSH-65 are much higher than those observed in sample WSH-95. Meanwhile, we report the first, to our knowledge, data showing such a highly positive relationship between Zn/Cd ratios and $\delta^{34}S_{CDT}$ values in sphalerite (WSH-95;R^2 = 0.96) from Zn-Pb deposits (Fig. 7); however, this correlation was not observed in sphalerite from sample WSH-65 (Fig. 6), suggesting different formation origins.

We summarized published Zn/Cd ratio and $\delta^{34}S_{CDT}$ data in sphalerite and observed the linear correlation between Zn/Cd ratios and $\delta^{34}S_{CDT}$ values at a large scale from the Fule deposit, where trends toward higher $\delta^{34}S_{CDT}$ values in later formed sphalerite that may be mirrored by increasing Zn/Cd ratios in the fluids with time (Fig. 7; Zhu et al., 2017). As mentioned above, multiple factors control the Zn/Cd ratios and $\delta^{34}S_{CDT}$ values in sphalerite. Indeed, based upon our data, it is impossible to unequivocally discern the key factors that result in such a strong positive correlation between Zn/Cd ratios and $\delta^{34}S_{CDT}$ values. However, fluid cooling process may be considered to account for the correlation between Zn/Cd ratios and $\delta^{34}S_{CDT}$ values. As discussed above, the sulfur signatures and Zn/Cd ratios in sphalerite have close relationships with fluid temperature (Machel et al. 1995; Strauss, 1997; Wen et al., 2016). The $\delta^{34}S_{CDT}$ values of sulfide would increase during the cooling of hydrothermal fluid (Rye and Ohmoto 1974; Thiessen et al. 2016; Zhu et al., 2017). Similarly, low temperatures unlikely favor Cd substitution in sphalerite under hydrothermal conditions (Schwartz, 2000; Wen et al., 2016), suggesting that sphalerite formed at low temperature has higher Zn/Cd ratio than the one formed at high temperature. These results demonstrate that both of Zn/Cd ratios and $\delta^{34}S_{CDT}$ values in sphalerite would increase during the cooling of hydrothermal fluid.

5.3. Implications

In the SYG area, Zn-Pb deposits were classified into MVT type deposits (Zhang et al., 2015, and reference therein) and Zn isotopic signatures in several Zn-Pb deposits in the SYG area have been well-defined, including the Tianbaoshan (+0.15 ~ +0.73‰, mean = 0.41‰; He et al., 2016), Shanshulin (0.00‰ ~ +0.55‰, mean = 0.25‰; Zhou et al., 2014a), Tianqiao (−0.26 ~ +0.58‰, mean = 0.26‰; Zhou et al., 2014b) and Banbanqiao (+0.07 ~ +0.71‰, mean = 0.42‰; Zhou et al., 2014b) deposits (Fig. 8). Although these deposits have different ranges of $\delta^{66}Zn$ values, the average $\delta^{66}Zn$ value of each deposit are concentrated in a narrow range from 0.26‰ to 0.42‰, similar to the initial $\delta^{66}Zn$ value of hydrothermal fluids during Ediacaran time. We present a possible model to explain such similar $\delta^{66}Zn$ values in both Zn-Pb deposits and hydrothermal fluids. Hydrothermal activities resulted in Zn pre-concentrated in sedimentary rocks (Dengying Formation), which might be a significant source bed for Zn-

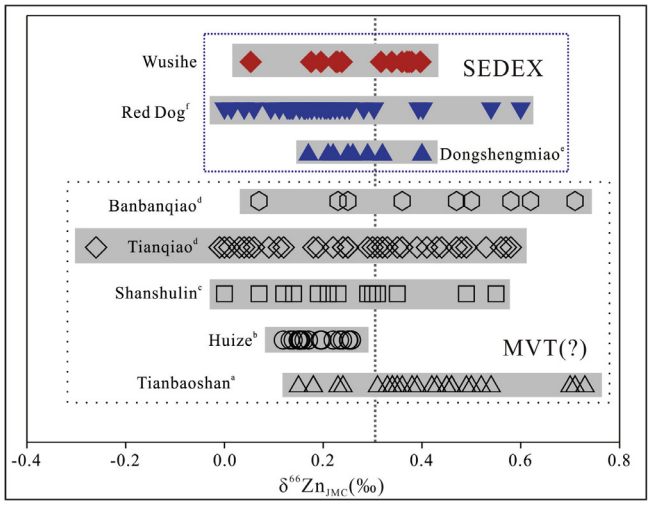

Fig. 8. Zn isotope compositions of sphalerite from different Zn-Pb deposits in the SYG area and from typical SEDEX deposits. The grey dash line is the estimated $\delta^{66}Zn$ value of Bulk Silicate Earth (0.28 ± 0.03‰; Chen et al., 2013). Data sources: [a]He et al. (2016); [b]Wu (2013); [c]Zhou et al. (2014a); [d]Zhou et al. (2014b); [e]Gao et al. (2017); and [f]Kelley et al. (2009).

Pb deposits in the SYG area, as suggested in previous studies (e.g., Wang et al., 2000; Zhou et al., 2014a). Thus, the measured δ^{66}Zn values of these deposits are similar. However, this hypothesis should be further tested with more detailed studies.

In a recomparison of the reported Zn isotope compositions of sphalerite from typical SEDEX type deposits, we found that the range of δ^{66}Zn values from the Wusihe deposit (0.05–0.40‰) is comparable to that of the Dongshengmiao deposit (0.17–0.40‰), but slightly smaller than that of the Red Dog deposit (0–0.6‰) (Fig. 8), suggesting similar Zn isotope signatures in SEDEX type deposits. Meanwhile, the estimated δ^{66}Zn value of hydrothermal fluid (0.37 ± 0.03‰) is similar to the middle range value of the Red Dog (0.30‰) and Dongshengmiao (0.29‰) deposits. It is proposed that the δ^{66}Zn value of hydrothermal fluid might be–0.37‰ in SEDEX hydrothermal systems.

Furthermore, sulfides, especially sphalerite, are the most abundant Zn-bearing mineral in hydrothermal systems. Our assessment provides additional constraints for Zn isotope fractionation during precipitation of sphalerite in hydrothermal fluids. On average, we found that the δ^{66}Zn value of hydrothermal fluids (0.37 ± 0.03‰), estimated in this study, is higher than that of previously reported value (< 0.3‰; Little et al., 2016). Recent studies have shown that sedimentary carbonates (~0.91‰) have much heavier Zn isotopic ratios than igneous rocks (~0.28‰) (Liu et al., 2016; Wang et al., 2017). Thus, the involvement of carbonates into the ore fluids could result in heavier δ^{66}Zn values in hydrothermal fluids. However, we have yet to evaluate the Zn contribution of sedimentary carbonates to hydrothermal fluids in the Wusihe deposit.

Generally, the average value of hydrothermal fluids is lower than that of seawater (~0.5‰; Little et al., 2016) but slightly higher than that of terrigenous materials (0.24 ± 0.06‰; Pichat et al., 2003), suggesting that Zn in sphalerite from the Wusihe deposit was possibly origined sourced from seawater and continental Zn. Meanwhile, we present the first effort to use Zn isotopes, preserved in syngenetic sphalerite, as proxies for hydrothermal activities in the Ediacaran Ocean (the Dengying Formation). We propose that Zn isotope compositions in paleo-ocean environments could be significantly affected by hydrothermal fluids, and thus, such effect should be elucidated when using Zn isotopes to reconstruct Zn isotopic compositions in the Ediacaran Ocean.

6. Conclusions

In this study, microdrilling system was employed for sphalerite collection from the stratigraphic base to the top of two hand specimens from the Wusihe deposit. We firstly investigated Zn and S isotopic compositions within these samples and evaluated Zn and S isotopic variations spatially and temporally during precipitation of sphalerite, in combination with Pb isotope compositions and Zn/Cd ratios in the same samples. The following observations and conclusions can be drawn:

(1) The $\delta^{34}S_{CDT}$ values of microdrilled sphalerite range from 9.4‰ to 20.9‰ (mean = 14.3‰), which are ca. 15‰ lower than that of sulfate from the Dengying Formation (mean = 29.6‰; Zhang et al., 2004; Goldberg et al., 2005). Previous studies have shown that MSR could result in much larger sulfur isotopic fractionation (up to 72‰) than that of TSR (< 20‰). It is thus that reduced sulfur in sphalerite formed via TSR, instead of MSR.
(2) There are no significant Zn isotopic fractionation from bottom to top of sample WSH-65 (Δ^{66}Zn = 0.08‰), however, the $\delta^{34}S_{CDT}$ values of microdrilled sphalerite vary from 13.2‰ to 20.9‰. We suggest that Zn isotopes are homogeneous in Zn-bearing hydrothermal fluids, and that Zn^{2+} was rapidly and completely precipitated to form sphalerite. This process could be used to explain the minor Zn isotopic variations in sphalerite, while fluid temperature variations may be the key factor that result in such large sulfur isotopic fractionation. In addition, we propose that initial hydrothermal fluid composition had δ^{66}Zn values of 0.37 ± 0.03‰.
(3) We observed positive linear relationships between δ^{66}Zn and $\delta^{34}S_{CDT}$ values and between $\delta^{34}S_{CDT}$ values and Zn/Cd ratios that have not been reported previously. Based upon previous studies, we propose that the kinetic fractionation of sulfur isotopes and partition of Zn and Cd during the formation of sphalerite are temperature dependent that lower fluid temperature could result in higher $\delta^{34}S_{CDT}$ values and Zn/Cd ratios in sphalerite, while higher fluid temperature could result in lower $\delta^{34}S_{CDT}$ values and Zn/Cd ratios.
(4) The δ^{66}Zn value of hydrothermal fluid (0.37 ± 0.03‰) is higher than that previously estimated (< 0.3‰; Little et al., 2016). We thus propose that the effects of hydrothermal activities on Zn isotope compositions should be elucidated when using Zn isotopes to reconstruct Zn isotopic compositions in the Ediacaran Ocean.

Acknowledgments

This project was financially supported by the National Key R&D Program of China (2017YFC0602503), National Natural Science Foundation of China (Nos. 41773012, 41503011), CAS “Light of West China” and the Science and Technology Foundation of Guizhou Province ([2016]1159). Journal reviewers are gratefully acknowledged for their helpful comments that allowed us to improve the manuscript.

References

Böttcher, M.E., Smock, A.M., Cypionka, H., 1998. Sulfur isotope fractionation during experimental precipitation of iron (II) and manganese (II) sulfide at room temperature. Chem. Geol. 146 (3), 127–134.
Chen, H., Savage, P.S., Teng, F.-Z., Helz, R.T., Moynier, F., 2013. Zinc isotope fractionation during magmatic differentiation and the isotopic composition of the bulk Earth. Earth Planet. Sci. Lett. 369, 34–42.
Cloquet, C., Carignan, J., Lehmann, M.F., Vanhaecke, F., 2008. Variation in the isotopic composition of zinc in the natural environment and the use of zinc isotopes in biogeosciences: a review. Anal. Bioanal. Chem. 390 (2), 451–463.
Deng, J., Wang, C., Bagas, L., Selvaraja, V., Jeon, H., Wu, B., Yang, L., 2016. Insights into ore genesis of the Jinding Zn–Pb deposit, Yunnan Province, China: Evidence from Zn and in-situ S isotopes. Ore Geol. Rev. http://dx.doi.org/10.1016/j.oregeorev.2016.10.036.
Duan, J., Tang, J., Lin, B., 2016. Zinc and lead isotope signatures of the Zhaxikang Pb Zn deposit, South Tibet: Implications for the source of the ore-forming metals. Ore Geol. Rev. 78, 58–68.
Fujii, T., Moynier, F., Pons, M.L., Albarède, F., 2011. The origin of Zn isotope fractionation in sulfides. Geochim. Cosmochim. Acta 75 (23), 7632–7643.
Gadd, M.G., Layton-Matthews, D., Peter, J.M., Paradis, S., Jonasson, I.R., 2017. The world-class Howard’s Pass SEDEX Zn-Pb district, Selwyn Basin, Yukon. Part II: the roles of thermochemical and bacterial sulfate reduction in metal fixation. Mineral. Deposita 52 (3), 405–419.
Gagnevin, D., Boyce, A.J., Barrie, C.D., Menuge, J.F., Blakeman, R.J., 2012. Zn, Fe and S isotope fractionation in a large hydrothermal system. Geochim. Cosmochim. Acta 88, 183–198.
Gao, Z., Zhu, X., Sun, J., Luo, Z., Bao, C., Tang, C., Ma, J., 2017. Spatial evolution of Zn-Fe-Pb isotopes of sphalerite within a single ore body: A case study from the Dongshengmiao ore deposit, Inner Mongolia, China. Miner. Deposita. http://dx.doi.org/10.1007/s00126-017-0724-x.
Goldberg, T., Poulton, S.W., Strauss, H., 2005. Sulphur and oxygen isotope signatures of late Neoproterozoic to early Cambrian sulphate, Yangtze Platform, China: diagenetic constraints and seawater evolution. Precambrian Res. 137 (3), 223–241.
Han, R.S., Liu, C.Q., Huang, Z.L., Chen, J., Ma, D.Y., Lei, L., Ma, G.S., 2007. Geological features and origin of the Huize carbonate-hosted Zn–Pb–(Ag) district, Yunnan, South China. Ore Geol. Rev. 31 (1–4), 360–383.
He, C.Z., Xiao, C.Y., Wen, H.J., Zhou, T., Zhu, C.W., Fan, H.F., 2016. Zb-S isotopic compositions of the Tianbaoshan carbonate-hosted Pb-Zn deposit in Sichuan, China: Implications for source of ore components. Acta Petrol. Sin. 32 (11), 3394–3406 (in Chinese with English abstract).
Huang, Z.L., Chen, J., Han, R.S., Li, W.B., Liu, C.Q., Zhang, Z.L., Ma, D.Y., Gao, D.R., Yang, H.L., 2004. Geochemistry and ore-formation of the Huize giant lead-zinc deposit, Yunnan Province, China: Discussion on the relationship between Emeishan flood basalts and lead-zinc mineralization (in Chinese). Geological Publishing House, Beijing, pp. 1–20.
John, S.G., Rouxel, O.J., Craddock, P.R., Engwall, A.M., Boyle, E.A., 2008. Zinc stable isotopes in seafloor hydrothermal vent fluids and chimneys. Earth Planet. Sci. Lett. 269 (1), 17–28.
Kelley, K.D., Wilkinson, J.J., Chapman, J.B., Crowther, H.L., Weiss, D.J., 2009. Zinc isotopes in sphalerite from base metal deposits on the Red Dog district, Northern Alaska. Econ. Geol. 104, 767–773.

Lefticariu, L., Behum, P.T., Bender, K.S., Lefticariu, M., 2017. Sulfur isotope fractionation as an indicator of biogeochemical processes in an AMD passive bioremediation system. Minerals 7 (3), 41.
Little, S.H., Vance, D., McManus, J., Severmann, S., 2016. Key role of continental margin sediments in the oceanic mass balance of Zn and Zn isotopes. Geology 44 (3), 207–210.
Liu, S.A., Wang, Z.Z., Li, S.G., Huang, J., Yang, W., 2016. Zinc isotope evidence for a large-scale carbonated mantle beneath eastern China. Earth Planet. Sci. Lett. 444, 169–178.
Liu, S.A., Wu, H.C., Shen, S.Z., Jiang, G.Q., Zhang, S.H., Lv, Y.W., Zhang, H., Li, S.G., 2017. Zinc isotope evidence for intensive magmatism immediately before the end-permian mass extinction. Geology 45 (4), 343–346.
Machel, H.G., Krouse, H.R., Sassen, R., 1995. Products and distinguishing criteria of bacterial and thermochemical sulfate reduction. Appl. Geochem. 10 (4), 373–389.
Mason, T.F.D., Weiss, D.J., Chapman, J.B., Wilkinson, J.J., Tessalina, S.G., Spiro, B., Horstwood, M.S.A., Spratt, J., Coles, B.J., 2005. Zn and Cu isotopic variability in the Alexandrinka volcanic-hosted massive sulphide (VHMS) ore deposit, Urals Russia. Chem. Geol. 221, 170–187.
Meshoulam, A., Amrani, A., 2017. Sulfur isotope exchange between thiophenes and inorganic sulfur compounds under hydrous pyrolysis conditions. Org. Geochem. 103, 79–87.
Pallavicini, N., Engström, E., Baxter, D.C., Öhlander, B., Ingri, J., Rodushkin, I., 2014. Cadmium isotope ratio measurements in environmental matrices by MC-ICP-MS. J. Anal. Atomic Spectrom. 29 (9), 1570–1584.
Pašava, J., Tornos, F., Chrastný, V., 2014. Zinc and sulfur isotope variation in sphalerite from carbonate-hosted zinc deposits, Cantabria Spain. Mineral. Deposita 49 (7), 797–807.
Pichat, S., Douchet, C., Albarède, F., 2003. Zinc isotope variations in deep-sea carbonates from the eastern equatorial Pacific over the last 175 ka. Earth Planet. Sci. Lett. 210 (1), 167–178.
Rollinson, H., 1993. Using Geochemical Data: Evaluation, Presentation, Interpretation. Copulished in the United States. John Wiley & Sons, Inc., New York, pp. 303–315.
Rosman, K.J.R., 1972. A survey of the isotopic and elemental abundances of zinc. Geochim. Cosmochim. Acta 36, 801–819.
Rye, R.O., Ohmoto, H., 1974. Sulfur and carbon isotopes and ore genesis: a review. Econ. Geol. 69, 826–842.
Schwartz, M.O., 2000. Cadmium in zinc deposits: economic geology of a polluting element. Int. Geol. Rev. 42, 445–469.
Strauss, H., 1997. The isotopic composition of sedimentary sulfur through time. Palaeogeogr. Palaeoclimatol. Palaeoecol. 132 (1), 97–118.
Tang, S.H., Zhu, X.K., Li, J., Yan, B., Li, S.Z., Li, Z.H., Wang, Y., Sun, J., 2016. New standard solutions for measurement of iron, copper and zinc isotopic compositions by multi-collector inductively coupled plasma-mass spectrometry. Rock Mineral Anal. 35 (2), 127–133 (in Chinese with English abstract).
Thiessen, E.J., Gleeson, S.A., Bennett, V., Creaser, R.A., 2016. The Tiger deposit: a carbonate-hosted, magmatic-hydrothermal gold deposit, Central Yukon, Canada. Econ. Geol. 111, 421–446.
Toutain, J.P., Sonke, J., Munoz, M., Nonell, A., Polvé, M., Viers, J., Freydier, R., Sortino, F., Joron, J.L., Sumarti, S., 2008. Evidence for Zn isotopic fractionation at Merapi volcano. Chem. Geol. 253, 74–82.
Wang, W. (2015). Texture and Structure Characteristics of Ore and Genetic Research of Wusihe Pb-Zn Deposit, Sichuan Province. A dissertation submitted to China University of Geosciences (Wuhan) for a master degree. Wuhan (In Chinese with English abstract).
Wang, X.C., Zhang, Z.R., Zheng, M.H., Xu, X.H., 2000. Metallogenic mechanism of the Tianbaoshan Pb-Zn deposit Sichuan. Chin. J. Geochem. 19 (2), 121–133 (in Chinese with English abstract).
Wang, W., Zhou, Z., Gong, Y., Xiong, S., 2014. Geological features and ore controlling factors of the wusihe lead-zinc deposit, Sichuan province. Acta Geol. Sin. (English Edition) 88 (z2), 209–210.
Wang, Z.Z., Liu, S.A., Liu, J., Huang, J., Xiao, Y., Chu, Z.Y., Zhao, X.M., Tang, L.M., 2017. Zinc isotope fractionation during mantle melting and constraints on the Zn isotope composition of Earth's upper mantle. Geochim. Cosmochim. Acta 198, 151–167.
Wen, H.J., Zhu, C.W., Zhang, Y.X., Cloquet, C., Fan, H.F., Fu, S.H., 2016. Zn/Cd ratios and cadmium isotope evidence for the classification of lead-zinc deposits. Sci. Rep. http://dx.doi.org/10.1038/srep25273.
Wilkinson, J.J., Weiss, D.J., Mason, T.F.D., Coles, B.J., 2005. Zinc isotope variation in hydrothermal systems: preliminary evidence from the Irish Midlands ore field. Econ. Geol. 100 (3), 583–590.
Wu, Y. (2013).The age and ore-forming process of MVT deposits in the boundary area of Sichuan-Yunnan-Guizhou provinces, Southwest China. A dissertation submitted to China University of Geosciences. Beijing (In Chinese with English abstract).
Xiong, G.Q., Jiang, X.S., Cui, X.Z., Zhuo, J.W., Lu, J.Z., Liu, J.H., Wang, Z.J., Wang, J., 2013. Strata location of the Lanbaoping Formation of the Proterozoic Ebian Group in the western Yangtze Block and its chronological evidence of zircon SHRIMP U-Pb age. Earth Sci. Front. 20 (4), 350–360 (In Chinese with English abstract).
Xiong, S.F., Yao, S.Z., Gong, Y.J., Tan, M.T., Zeng, G.P., Wang, W., 2016. Ore-forming fluid and thermochemical sulfate reduction in the Wusihe lead-zinc deposit, Sichuan Province China. Earth Sci. 41 (1), 105–120 (In Chinese with English abstract).
Ye, L., Cook, N.J., Ciobanu, C.L., Liu, Y.P., Zhang, Q., Liu, T.G., Gao, W., Yang, Y.L., Danyushevskiy, L., 2011. Trace and minor elements in sphalerite from base metal deposits in South China: a LA-ICPMS study. Ore Geol. Rev. 39 (4), 188–217.
Yuan, H.L., Yuan, W.T., Cheng, C., Liang, P., Liu, X., Dai, M.N., Bao, Z., Zong, C.L., Chen, K.Y., Lai, S.C., 2016. Evaluation of lead isotope compositions of NIST NBS 981 measured by thermal ionization mass spectrometer and multiple-collector inductively coupled plasma mass spectrometer. Solid Earth Sci. 1 (2), 74–78.
Zaw, K., Peters, S.G., Cromie, P., Burrett, C., Hou, Z., 2007. Nature, diversity of deposit types and metallogenic relations of South China. Ore Geol. Rev. 31 (1–4), 3–47.
Zhang, T.G., Chu, X.L., Zhang, Q.R., Feng, L.J., Huo, W.G., 2004. The sulfur and carbon isotopic records in carbonates of the Dengying Formation in the Yangtze Platform China. Acta Petrol. Sin. 20 (3), 717–724.
Zhang, C.Q., Wu, Y., Hou, L., Mao, J.W., 2015. Geodynamic setting of mineralization of Mississippi Valley-type deposits in world-class Sichuan–Yunnan–Guizhou Zn–Pb triangle, southwest China: Implications from age-dating studies in the past decade and the Sm–Nd age of Jinshachang deposit. J. Asian Earth Sci. 103, 103–114.
Zheng, Z. X. (2012). Geological features and genesis of Wusihe Pb-Zn deposit, Sichuan. A dissertation submitted to Chang'an University for a master degree. Xi'an (In Chinese with English abstract).
Zhou, C.X., Wei, C.S., Guo, J.Y., Li, C.Y., 2001. The source of metals in the Qilinchang Zn-Pb deposit, northeastern Yunnan, China: Pb-Sr isotope constraints. Econ. Geol. 96 (3), 583–598.
Zhou, J.X., Huang, Z.L., Lv, Z.C., Zhu, X.K., Gao, J.G., Mirnejad, H., 2014a. Geology, isotope geochemistry and ore genesis of the Shanshulin carbonate-hosted Pb–Zn deposit, southwest China. Ore Geol. Rev. 63, 209–225.
Zhou, J.X., Huang, Z.L., Zhou, M.F., Zhu, X.K., Muchez, P., 2014b. Zinc, sulfur and lead isotopic variations in carbonate-hosted Pb–Zn sulfide deposits, southwest China. Ore Geol. Rev. 58, 41–54.
Zhu, C.W., Wen, H.J., Zhang, Y.X., Fan, H.F., Fu, S.H., Xu, J., Qin, T.R., 2013. Characteristics of Cd isotopic compositions and their genetic significance in the lead–zinc deposits of SW China. Sci. China Earth Sci. 56, 2056–2065.
Zhu, C.W., Wen, H.J., Zhang, Y.X., Fan, H.F., 2016. Cadmium and sulfur isotopic compositions of the Tianbaoshan Zn–Pb–Cd deposit, Sichuan Province, China. Ore Geol. Rev. 76, 152–162.
Zhu, C.W., Wen, H.J., Zhang, Y.X., Fu, S.H., Fan, H.F., Cloquet, C., 2017. Cadmium isotope fractionation in the Fule Mississippi Valley-type deposit Southwest China. Mineral. Deposita 52 (5), 675–686.